Accepted Author Manuscript (AAM)

Article Title: Enhancing hydroxychloroquine detection using carbon paste electrode modified with platinum nanoparticles and MWCNTs

Authors: Maria H. A. Feitosa, Anderson M. Santos, Ademar Wong, Maria D. P. T. Sotomayor, Willyam R. P. Barros, Marcos R. V. Lanza, Fernando C. Moraes

Journal: *Journal of Applied Electrochemistry*

DOI: https://doi.org/10.1007/s10800-025-02293-2

Received: 18 December 2024
Accepted: 02 March 2025
Published online: 11 March 2025

Enhancing hydroxychloroquine detection using carbon paste electrode modified with platinum nanoparticles and MWCNTs

Maria H. A. Feitosa[1], Anderson M. Santos[2*], Ademar Wong[3], Maria D. P. T. Sotomayor[3], Willyam R. P. Barros[4], Marcos R. V. Lanza[2], Fernando C. Moraes[1**]

[1]Department of Chemistry, Federal University of São Carlos (UFSCar), 13560-970, São Carlos, SP, Brazil.

[2]São Carlos Institute of Chemistry, University of São Paulo (USP), 13566-590, São Carlos, SP, Brazil.

[3]Institute of Chemistry, State University of São Paulo (UNESP), 14801-970, Araraquara, SP, Brazil.

[4]Federal University of Grande Dourados (UFGD), 79804-970, Dourados, MS, Brazil.

Corresponding author[*,**]:

E-mail address: Anderson M. Santos (andersonmartinsts@gmail.com)

Fernando C. Moraes (fcmoraes@ufscar.br)

Graphical Abstract

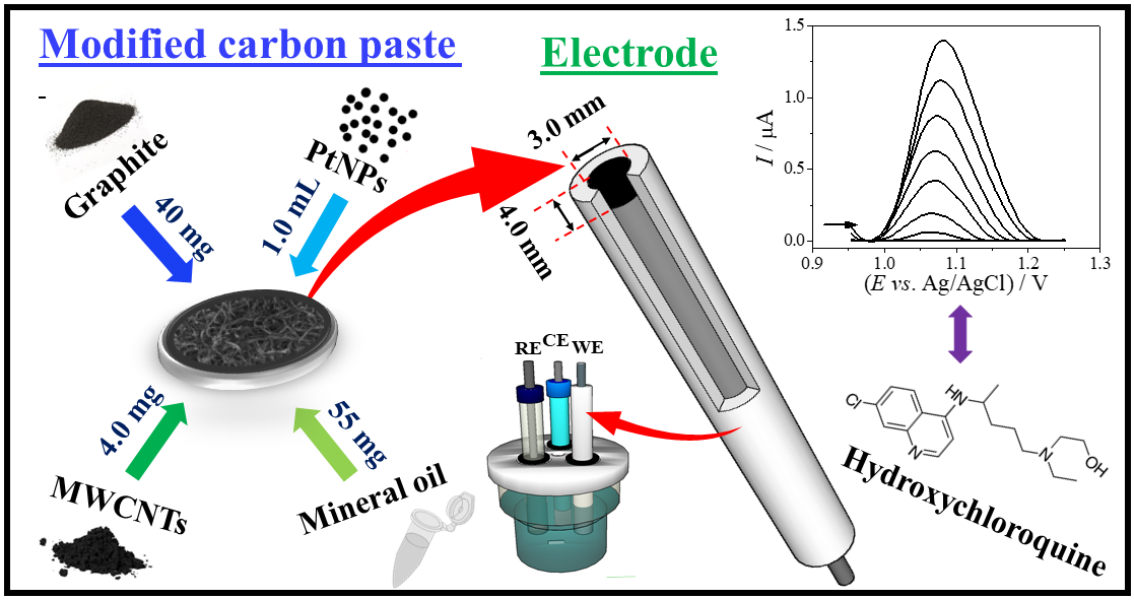

"Schematic representation of the fabrication of a carbon paste electrode modified with carbon nanotubes and platinum nanoparticles, and its application in the determination of hydroxychloroquine in urine, serum, and river water samples using square wave voltammetry".

Abstract

In this study, a carbon paste electrode (CPE) modified with multi-walled carbon nanotubes (MWCNTs) and platinum nanoparticles (Pt NPs) was developed for the detection of hydroxychloroquine in environmental and biological samples. The electrodes defined as MWCNTs/CPE and Pt NPs-MWCNTs/CPE, were subjected to characterization analyses, where their structural and morphological properties were investigated. The electrochemical measurements were carried out using cyclic and square wave voltammetry techniques. Under optimal conditions, the proposed sensor displayed a linear concentration range of 0.099 - 7.1 μmol L^{-1} (n = 3) in 0.10 mol L^{-1} phosphate buffer solution at pH 6.0, with detection and quantification limits of 28 nmol L^{-1} and 93 nmol L^{-1}, respectively. The selectivity of the proposed sensor toward hydroxychloroquine detection was verified in the presence of potential interferents such as uric acid, glucose, urea, ascorbic acid, albumin, metals, and humic acid. For the analysis of its applicability, the sensor was successfully applied for hydroxychloroquine detection in biological and environmental samples, where the results obtained were comparable to those obtained under spectrophotometry (reference method), thus confirming the feasibility of the method. The findings of this study show that the proposed sensor exhibits exceptional performance and is suitable for use in the detection of pharmaceuticals in different real matrices.

Keywords: Modified electrode; Carbon paste electrode; Platinum nanoparticles; Carbon nanotube; Hydroxychloroquine.

1. Introduction

The development and application of electrochemical sensors for the determination of biologically active compounds have been an object of extensive studies in analytical chemistry over the past few decades; these sensors are increasingly being explored for the determination of different compounds of emerging concern including pharmaceuticals, dyes, plastic additives, pesticides, among other compounds of equal and/or higher toxicity [1-3].

Over the past few decades, the rapid and increasing progress we have witnessed in the research on electrochemical sensors has been intrinsically linked to the growth of nanotechnology [4]. Nanoscale miniaturization has helped us improve the morphologies and dimensions of conductive and semiconductor materials, which are crucial for the enhancement of electrochemical signals through conductive properties, as well as catalytic and chemical interactions on functional surfaces [4,5].

At the same time, several materials have been widely investigated for application in the detection and quantification of organic and inorganic compounds that are of environmental concern. Of these materials, semiconductors, metallic nanoparticles and carbon-based materials have become remarkably popular among researchers due to their outstanding efficiency and performance, with the latter found to exhibit the best electrochemical properties owing to its ability to facilitate redox processes. Some notable examples of carbon-based materials include carbon black, graphite, graphene, nanotubes, nanofibers, activated carbon, biochar and quantum dots [6-8].

Taking the above considerations into account, carbon paste electrodes (CPE) have become increasingly popular due to their several outstanding advantages; these advantages include rapid surface renewal, low cost of production, high selectivity, low residual current, and high porosity [9-11]. These attributes make CPEs particularly suitable for use in drug detection, where the graphite paste acts as a catalyst in electron

transfer, contributing effectively toward the reduction of resistance in redox processes [12]. Furthermore, the surface of CPEs can be modified with other materials, mainly carbon-based materials and nanoparticles, where the modifying agents help maximize the generation of active catalytic sites, due to the high surface to volume ratio of these structures [13]. Carbonaceous materials, such as carbon nanotubes (CNTs), consisted of a graphene sheet rolled into a cylindrical structure with hemispherical ends, and are classified as either single-walled carbon nanotubes (SWCNTs) and multi-walled carbon nanotubes (MWCNTs) depending on the number of graphene layers [14]. CNTs possess high conductivity, large surface area, and the ease of functionalization for chemical and biological species immobilization, make them ideal for use in electrochemical sensors. These properties enable more sensitive detections with lower detectability compared to other materials [15,14,16].

The production of nanocomposites containing carbonaceous materials, especially in combination with conductive nanoparticles such as platinum nanoparticles (Pt NPs), presents a promising approach for the development of sensors that are suitable and highly efficient for compounds detection [17-19]. Pt NPs exhibit exceptional properties, which include high surface to volume ratio, high adsorptive capacity, superior catalytic activity and small dimensions. These features make Pt NPs essential for use in the detection of electroactive molecules, as they help us obtain a fast and sensitive response [20,21].

One of the major organic compounds of huge environmental concern is hydroxychloroquine (HCQ); this drug is widely used in the prevention and treatment of malaria. In addition, HCQ is employed in the management of auto-immune diseases such as rheumatoid arthritis, lupus erythematosus, cutaneous porphyria, and photosensitive diseases [22,23].

In Brazil, malaria is largely endemic, with more than 100,000 infected cases annually; this makes HCQ a drug of recurrent use, with high potential for release/disposal into the environment [24-26]. Another point worth mentioning is that, during the COVID-19 pandemic, many countries, including Brazil, used the HCQ drug in the early treatment of the coronavirus, even before science validated its efficacy or suitable vaccines were discovered/produced [27]. And despite the fact that scientific evidence proved that HCQ was ineffective against the coronavirus, its use persisted for quite some time [28,29]. The continuous widespread use of HCQ globally has resulted in its rampant disposal into the environment, and this poses serious risks to both human health and the ecosystems. This highlights the need to develop and enhance detection techniques that can effectively determine the presence of the compound in real samples. Standard methods for determining HCQ include electrophoresis [30], spectrophotometry [31], spectrofluorimetry [32], and high-performance liquid chromatography (HPLC) [33,34]. However, alternative methods such as electrochemical techniques have emerged and gained increasing popularity among researchers [35-37].

Therefore, the present study aimed to develop a carbon paste electrode modified with MWCNTs and Pt NPs for the sensitive and selective electrochemical determination of HCQ in aqueous samples including urine, river water, and bovine serum.

2. Experimental

2.1. Reagents and solutions

Graphite powder, mineral oil, bovine serum, hexachloroplatinium (IV) (H_2PtCl_6), sodium borohydride ($NaBH_4$), chitosan (CTS), HNO_3, H_2SO_4, graphite powder, and multiwalled carbon nanotubes (MWCNTs) were purchased from Sigma-Aldrich (Missouri, USA). HCQ was obtained from the compounding pharmacy Calendula situated in São Carlos (São Paulo, Brazil). The salts (KH_2PO_4, K_2HPO_4, and K_3PO_4),

149 which were used to prepare 0.10 mol L^{-1} phosphate buffer solution (PBS), in addition to
150 potassium chloride (KCl), were supplied by Synth (São Paulo, Brazil). The solutions were
151 rigorously prepared with ultrapure water, with resistivity ≥ 18.0 MΩ cm, obtained through
152 a Milli-Q Direct-0.3 purification system (Billerica, USA). All reagents used in this study
153 were of analytical grade, with purity greater than 99%; this helped ensure the reliability
154 and accuracy of the experimental results. Stock solutions of
155 0.010 mol L^{-1} HCQ were prepared directly in ultrapure water.
156
157 *2.2.Apparatus*
158 The electrochemical experiments were performed using an Autolab PGSTAT12
159 potentiostat/galvanostat (Herisau, Switzerland) controlled by the GPES 4.9 software. The
160 experimental system consisted of a 10.0 mL electrochemical cell equipped with three
161 electrodes: Ag/AgCl (3.0 mol L^{-1} KCl) − used as a reference electrode, a platinum plate
162 (A = 1.0 cm^2) used as a counter electrode, and the bare or modified CPE, which was used
163 as the working electrode (Ø = 3.0 mm).
164 The morphological characterization of the CPE, MWCNTs/CPE and Pt NPs-
165 MWCNTs/CPE was performed by scanning electron microscopy (SEM), using a Hitachi
166 microscope model S-4800 (Kyoto, Japan). The analysis of the optical absorption of the
167 samples (river water, serum and synthetic urine) was performed by UV-vis
168 spectrophotometry using a Shimadzu spectrophotometer model UV 2550 (Kyoto, Japan).
169
170 *2.3.* Synthesis of the Pt NPs
171 The Pt NPs were synthesized based on the method described by Deng *et al.* [38];
172 this method consisted of the reduction of H_2PtCl_6 in the presence of CTS - used as a
173 stabilizing agent, and sodium borohydride ($NaBH_4$) - used as the reducing agent. Initially,

24 mL of a 0.10 % (m/v) CTS solution was mixed with 1.0 mL of a 2.0×10^{-2} mol L^{-1} H_2PtCl_6 and kept under stirring for 30 min. Subsequently, 0.50 mL of a 0.40 mol L^{-1} $NaBH_4$ solution was gradually added to the mixture, promoting the reduction of the dispersed species in the solution. The dispersion obtained was then stored in an amber bottle for later use.

2.4. Preparation of the CPE, MWCNTs/CPE and Pt NPs-MWCNTs/CPE sensor

The MWCNTs was functionalized according to the method described by Wong *et al.* [39], using a 3:1 (v/v) mixture of concentrated sulfuric (H_2SO_4) and nitric (HNO_3) acids. The bare CPE sensor was prepared using only graphite powder and mineral oil. Then, the MWCNTs/CPE sensor was prepared using graphite powder, mineral oil and MWCNTs. Finally, the Pt NPs-MWCNTs/CPE sensor was produced by mixing Pt NPs, MWCNTs, graphite powder and mineral oil in different proportions. The best composition obtained consisted of 1.0 mL of the Pt NPs solution, 40 mg of graphite powder, 4.0 mg MWCNTs and 3 drops (approximately 55 mg) of mineral oil. Initially, the Pt NPs solution, graphite powder, and MWCNTs were mixed and left to dry in an oven. After drying, the mineral oil was added therein, leading to the formation of the paste, as shown in Scheme 1. The modified carbon paste was inserted into a cylindrical Teflon® tube, where it was compacted against a smooth surface and then polished on clean paper in order to have a homogeneous and well-compacted surface.

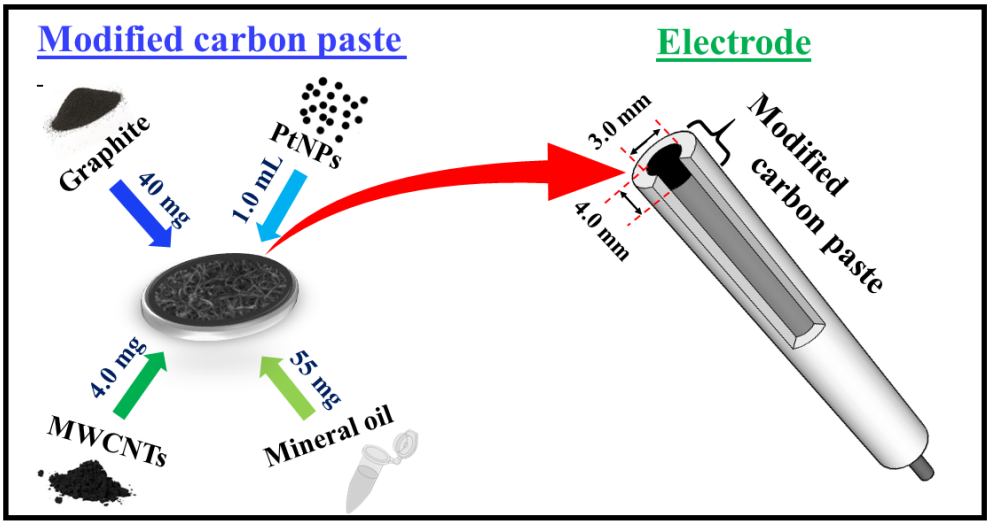

Scheme 1. Preparation scheme of the modified CPE.

2.5.Preparation of the samples

Synthetic urine samples were prepared as proposed by Laube *et al.* [40]. The preparation was done by adding 0.20 mmol L^{-1} KCl, 0.18 mmol L^{-1} NH_4Cl, 0.10 mmol L^{-1} NaCl, 0.10 mmol L^{-1} $CaCl_2$, 0.15 mmol L^{-1} KH_2PO_4 and 0. 18 mmol L^{-1} of urea into a 25 mL volumetric flask, and mixing the content with ultrapure water. Commercial bovine serum sample was used directly, without any pre-treatment procedures. The river water sample was collected from the Monjolinho river (São Carlos, São Paulo, Brazil); the collection point was recorded using the Global Positioning System (21°59'10.5"S 47°52'52.2"W). This sample was collected using a flask attached to a rod, transferred to amber polyethylene vials, and stored in a refrigerator at a temperature of approximately 3.0 °C.

Subsequently, each sample (urine, serum and river water) was transferred into 10 mL flasks, to which different aliquots of 1.0 mmol L^{-1} HCQ standard solutions were carefully added. Finally, 300 µL of the sample was placed in the electrochemical cell, completed with the supporting electrolyte (PBS at pH 6.0), and analyzed for recovery study.

3. Results and discussion

3.1. Morphological characterization of the materials

The morphological characterization of the MWCNTs and Pt NPs, used in the modification of the CPE, was performed by scanning electron microscopy (SEM). Fig. 1 presents the SEM images of the MWCNTs/CPE obtained at different magnifications (A-C). The images reveal the characteristic structure of the nanotubes, where a cluster of nanotubes can be found dispersed in the graphitic material. Fig. 1D and 1E exhibit the structure of the CPE modified with MWCNTs and Pt NPs, evidenced by the multiple spheres dispersed throughout the material. Additionally, Fig. 1E (inset) shows the EDS diagram, which confirms the formation of the Pt NPs structure; the nanoparticle structure has an average diameter of 4.4 nm, as illustrated in Fig. 1F. The small size of the Pt NPs results in a high surface to volume ratio, which contributes toward enhancing the electrochemical activity and sensitivity of the Pt NPs-MWCNTs/CPE sensor.

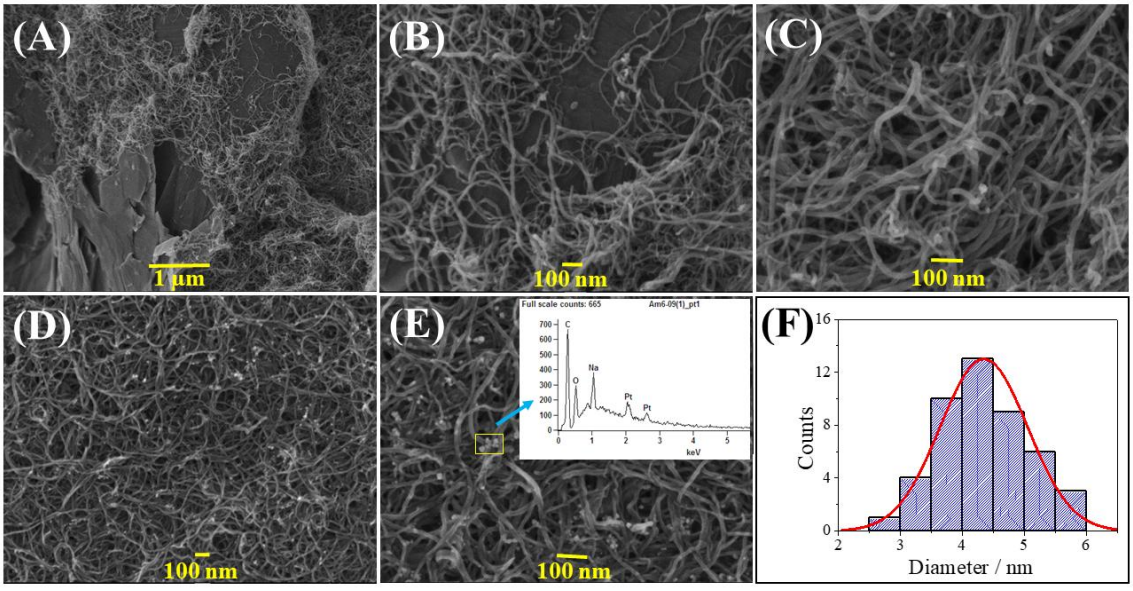

Fig. 1. SEM images for MWCNTs/CPE composite **(A – C),** Pt NPs-MWCNTs/CPE sensor **(D – E)**, and histogram for Pt NPs (**F**). Inset of Fig. E: EDS to Pt NPs.

232

233 *3.2. Determination of the electroactive area*

234 The electroactive area of the CPE, MWCNTs/CPE, and Pt NPs-MWCNTs/CPE
235 was estimated using the Randles-Sevcik equation (1) below [41]. This analysis was
236 performed by cyclic voltammetry (CV), at the scan rate ranging from 10 to 100 mV s^{-1},
237 using 0.10 mol L^{-1} KCl solution in the presence of 1.0 mmol L^{-1} $[Fe(CN)_6]^{3-}$ (Fig. S1A
238 – C), and a comparison between the different sensors is shown in Fig. S1D (50 mV s^{-1}).

239

240 $$I_p = \pm (2.69 \times 10^5)\, n^{3/2} A\, D^{1/2}\, C\, v^{1/2} \quad \text{(Eq. 1)}$$

241

242 where I_p is the peak current, n is the number of electrons transferred, A is the electroactive
243 area (cm^2), D is the diffusion coefficient of $[Fe(CN)_6]^{3-}$ in a 0.10 mol L^{-1} KCl solution
244 (7.6×10^{-6} cm^2 s^{-1}), C is the $[Fe(CN)_6]^{3-}$ concentration (mol cm^{-3}), and v is the scan rate
245 (V s^{-1}).

246 As shown in Fig. S1E, the slopes obtained from the I_p *vs.* $v^{1/2}$ plots for the process
247 involving the oxidation of $[Fe(CN)_6]^{3-}$ were 2.38×10^{-5}, 4.22×10^{-5}, and 6.34×10^{-5} A
248 $V^{-1/2}$ $s^{1/2}$ for the CPE, MWCNTs/CPE and Pt NPs-MWCNTs/CPE, respectively. The
249 corresponding electroactive areas recorded for the CPE, MWCNTs/CPE and Pt NPs-
250 MWCNTs/CPE were 0.032, 0.057, and 0.085 cm^2, respectively. Based on these results,
251 we can conclude that the electrochemical response of the $[Fe(CN)_6]^{3-}$ probe is
252 significantly influenced by modifications to the CPE. In this way, it is clear that the use
253 of the Pt NPs-MWCNTs-modified CPE led to a 2.7-fold increase in the electroactive area
254 compared to the unmodified CPE.

255 *3.3. Electrochemical characterization*

256 Electrochemical impedance spectroscopy (EIS) was performed at open circuit
257 potential (OCP) in 0.10 mol L^{-1} KCl solution, in the presence of 1.0 mmol L^{-1} of

258 $[Fe(CN)_6]^{3-/4-}$ employed as redox probe. This technique is an effective tool for
259 characterizing electron transfer properties at the solution/electrode interface. Fig. 2
260 presents the Nyquist plots obtained in the frequency range of 100 kHz to 1.0 Hz for the
261 CPE, MWCNTs/CPE, and Pt NPs-MWCNTs/CPE. The plots exhibit a distinct two-
262 component behavior, characterized by a semi-circular and a linear region. The linear
263 interval is attributed to the diffusion-controlled mass transport of electroactive species,
264 while the semi-circle reflects charge-transfer limitations, with the diameter correlating
265 with the charge-transfer resistance (R_{ct}); in other words, a larger semi-circle indicates a
266 higher R_{ct}.

267 The inset of Fig. 2 shows the Randles (adapted) equivalent circuit derived from
268 the analysis of the respective electrodes investigated. This circuit consists of the solution
269 resistance (R_s) in series with a constant phase element (*CPE*), in a parallel combination
270 of the R_{ct} and Warburg impedance (*W*). Based on our calculations, R_{ct} values of 6.31, 5.17
271 and 4.25 KΩ were obtained for the CPE, MWCNTs/CPE and Pt NPs-MWCNTs/CPE,
272 respectively. It is evident that for the modified electrodes, there was a decrease in the size
273 of the semi-circle, and this led to a reduction in R_{ct}, which reflected an increase in
274 electrode conductivity.

275

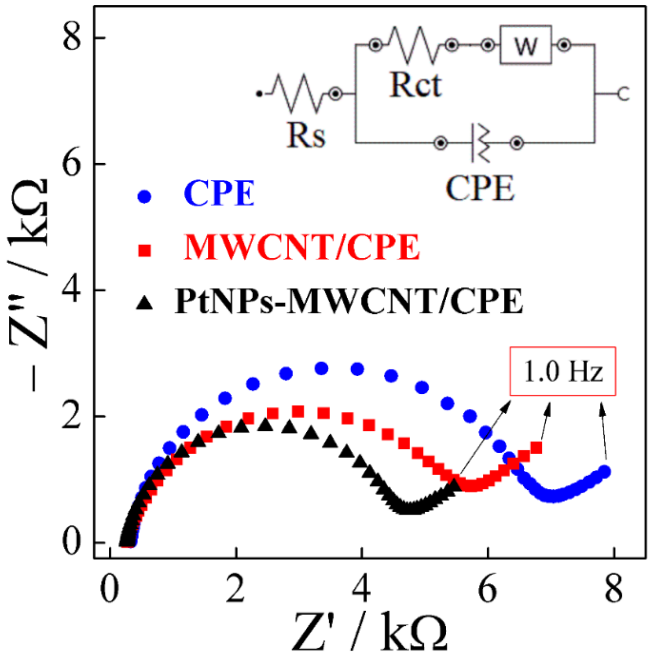

Fig. 2. EIS diagrams based on the application of CPE (blue), MWCNTs/CPE (red) and Pt NPs-MWCNTs/CPE (black) using 0.10 mol L^{-1} KCl containing 1.0 mmol L^{-1} $[Fe(CN)_6]^{3-/4-}$ and frequency range of 100 KHz to 1.0 Hz. Inset: Respective equivalent circuit.

Subsequently, the EIS data was also used to calculate the apparent heterogeneous electron transfer rate constant (k^0) using equation 2 (Eq. 2)[42,43].

$$K^0 = \frac{RT}{F^2 R_{ct} A C} \quad \text{(Eq. 2)}$$

where k^0 is the standard heterogeneous electron transfer rate constant (cm s^{-1}), R is the universal gas constant (8.314 J K^{-1} mol^{-1}), T is the temperature (298.15 K), F is the Faraday constant (96,485 C mol^{-1}), R_{ct} is the electron transfer resistance (Ω), A is the electrode surface area (cm^2), and C is the concentration of the $[Fe(CN)_6]^{3-/4-}$ solution (1.0 mmol cm^{-3}).

The k^0 values recorded for the CPE, MWCNTs/CPE and Pt NPs-MWCNTs/CPE were 6.03×10^{-4}, 7.36×10^{-4}, and 8.95×10^{-4} cm s^{-1}, respectively. The k^0 values serve as indicators of the kinetic facility/behavior of the redox pair involved. A lower k^0 value

indicates a slower reaction kinetics, which results in a longer equilibration time. On the other hand, a higher k^0 corresponds to faster reaction kinetics, which leads to a more rapid equilibration. In the present study, the Pt NPs-MWCNTs/CPE sensor exhibited a higher k^0 value compared to the other electrodes. This suggests that the Pt NPs-MWCNTs/CPE facilitates a more rapid electron transfer process, leading to enhanced redox reaction kinetics.

3.4. Electrochemical behavior of HCQ

Initially, cyclic voltammetry (CV) was used to evaluate the electrochemical behavior of the HCQ molecule using different electrodes (CPE, MWCNTs/CPE, and Pt NPs-MWCNTs/CPE) over the potential range of +0.30 to +1.4 V. Fig. 3A shows the cyclic voltammograms (50 mV s^{-1}) recorded for 0.10 mol L^{-1} PBS (at pH 6.0) containing 0.10 mmol L^{-1} HCQ. The results obtained showed that the compound exhibited two distinct oxidation peaks at approximately 0.9 and 1.2 V. This finding is in agreement with previous studies that have also pointed out the presence of these distinct peaks which are possibly related to the deprotonation of the amine and hydroxyl groups [23,44]. Remarkably, no reduction peaks were observed during the cathodic scan; this outcome shows that the oxidation reaction is wholly irreversible.

In addition to CV, the behavior of the HCQ compound was analyzed using square wave voltammetry (SWV) (Fig. 3B). The electrochemical responses obtained for each electrode were found to be consistent with the CV results. As illustrated in Fig. 3A and B, the Pt NPs-MWCNTs/CPE sensor presented higher oxidation peak current (I_{pox}) values compared to the unmodified CPE and the CPE modified with MWCNTs only. The Pt NPs-MWCNTs composite significantly enhances the electroactive surface area of the CPE, leading to improved sensitivity for HCQ detection in aqueous media. The porous

318 structure of the MWCNTs network provides a favorable platform for Pt NPs
319 immobilization; this facilitates electron transfer kinetics and promotes a synergistic effect
320 between the two components, leading to improvements in the electrochemical detection
321 of HCQ [45]. Thus, the Pt NPs-MWCNTs-modified carbon paste electrode was selected
322 for the conduct of subsequent HCQ detection studies.

323

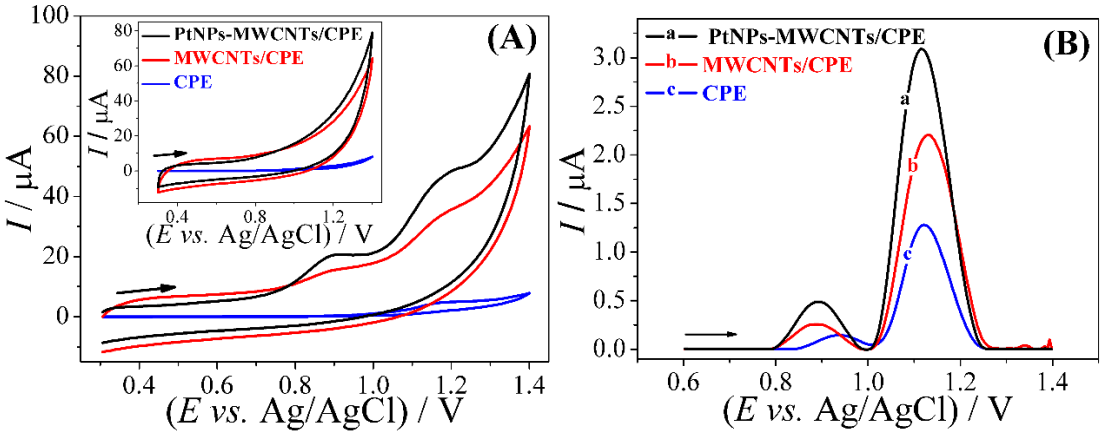

324

325 **Fig. 3. (A)** Cyclic voltammograms (50 mV s^{-1}) for 0.10 mmol L^{-1} of HCQ (blank
326 measurements inserted) and **(B)** square wave voltammograms for 50 µmol L^{-1} of HCQ,
327 both in 0.10 mol L^{-1} PBS at pH 6.0 using CPE (–), MWCNTs/CPE (–) and Pt NPs-
328 MWCNTs/CPE (–).

329

330 *3.5. Optimization of analytical parameters*

331 The effect of H^+ ion concentration on the reaction involving HCQ oxidation was
332 investigated using SWV in 0.10 mol L^{-1} PBS, with adjustments in pH from 4.0 to 9.0. As
333 shown in Fig. 4, the optimum pH of the supporting electrolyte, which resulted in the
334 largest peak current, was 6.0; thus, this condition was used in the subsequent experiments.
335 The peak potential (E_p) for HCQ oxidation exhibited a linear shift towards more negative
336 values as the pH increased from acidic to alkaline conditions, indicating the involvement
337 of protons in the electrooxidation of HCQ. The inset graph in Fig. 4 shows the correlation

between the E_p and pH, where one can see the presence of a linear trend with a slope of –0.057 V pH^{-1}. This slope is in close agreement with the theoretical value predicted by the Nernst equation of –0.0592 V pH^{-1}, which is typical of redox reactions involving the transfer of an equal number of electrons and protons [41]. This result is in line with previous studies on HCQ electro-oxidation which have demonstrated that the process is characterized by the transfer of two electrons and two protons [23,46]. The proposed reaction mechanism involving the electro-oxidation of the HCQ molecule is illustrated in Scheme 2:

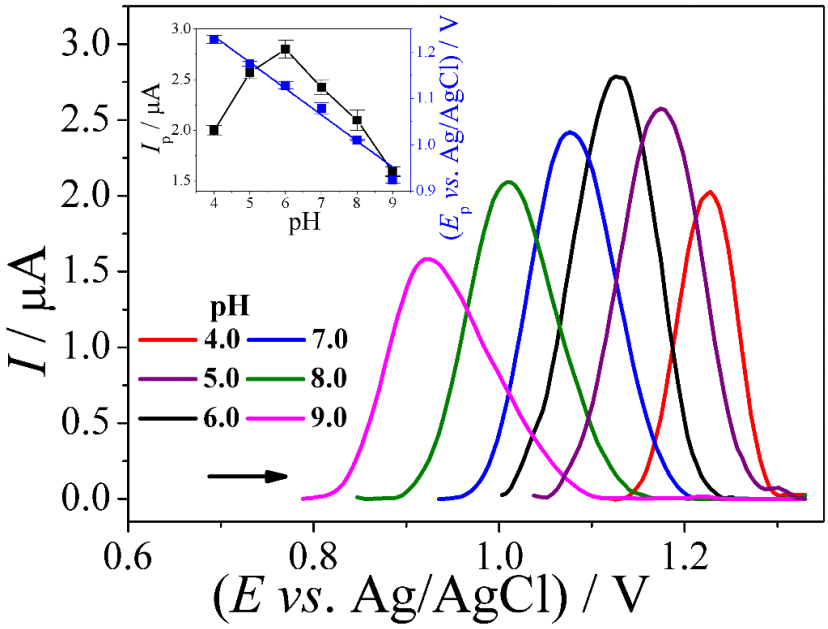

Fig. 4. SW voltammograms recorded for 50 µmol L^{-1} HCQ using 0.10 mol L^{-1} PBS with pH ranging from 4.0 to 9.0 using the Pt NPs-MWCNTs/CPE sensor. Parameters: f = 15 Hz, a = 40 mV and ΔE_s = 5 mV s^{-1}. Inset: E_p *vs.* pH and I_p *vs.* pH.

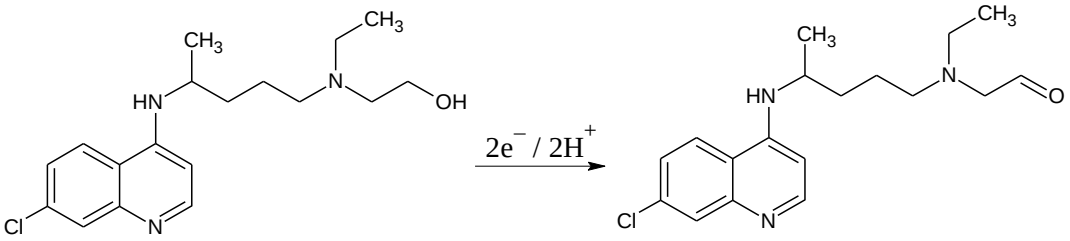

Scheme 2 – Proposed electrode reaction in HCQ oxidation.

Next, the number of electrons (n_e) was estimated using CV at a scan rate of 50 mV s^{-1}, using Eq. 3.

$$E_p - E_{p/2} = \frac{47.7}{(\alpha \times n_e)} \text{mV} \quad \text{(Eq. 3)}$$

In this analysis, the difference between the peak potential and the half-peak potential ($E_p - E_{p/2}$) was 57 mV. The electron transfer coefficient (α) was assumed to be 0.5, a value typical for fully irreversible reactions [41]. Substituting these values into the Eq. 3 resulted in a calculated n_e value of 1.7, which is close to 2. This result is consistent with the E_p versus pH analysis, which suggested a two-electron mechanism for the second peak in the electro-oxidation of the HCQ molecule.

Subsequently, we evaluated the effectiveness of PBS and Briton-Robson (BR) buffer solution, both at pH 6.0, when applied as supporting electrolytes (Fig. S2). These electrolytes were selected due to their widespread and frequent use in electrochemical detection systems for various analyte, such as pharmaceutical compounds. The results of this analysis showed that the PBS exhibited a greater peak current compared to BR; as such, PBS was chosen for the conduct of subsequent experiments. Finally, the analytical parameters, including amplitude (a), frequency (f), and potential increment (ΔE_s), which

exert influence over the SWV response were optimized. In addition to the aforementioned parameters, the accumulation time (t_{acc}) was also optimized. The optimal values obtained for the parameters were f = 15 Hz, a = 50 mV, ΔE_s = 5 mV, and t_{acc} = 30 s (see Table S1 in the SI).

3.6. Effect of scan rate

The electrochemical behavior of the Pt NPs-MWCNTs/CPE sensor was also investigated taking into account the scan rate effect. For this analysis, CV was applied at scan rates ranging from 10 to 100 mV s^{-1} using 0.10 mol L^{-1} PBS, at pH 6.0, as supporting electrolyte, in the presence of 0.10 mmol L^{-1} HCQ. As can be observed in Fig. 5A, an increase in scan rate resulted in a linear increase in peak current magnitude. The analysis of the relationship between peak current and scan rate (ΔI_p *vs.* v), as well as between peak current and the square root of scan rate (ΔI_p *vs.* $v^{1/2}$) (Fig. 5B and C) pointed to a good linearity between these elements; this outcome is indicative of an electrochemical process controlled by diffusion and/or adsorption [41]. To help elucidate the dominant process involved, the relationship between the logarithm of peak current and the logarithm of scan rate ((log I_p *vs.* log v) was also evaluated (Fig. 5D); this analysis resulted in the slope value of 0.58, which is close to the theoretical value of 0.5 and found to be typically characteristic of diffusion-controlled processes [41,47]. These findings support the hypothesis that mass transport of the HCQ to the electrode surface is primarily governed by diffusion.

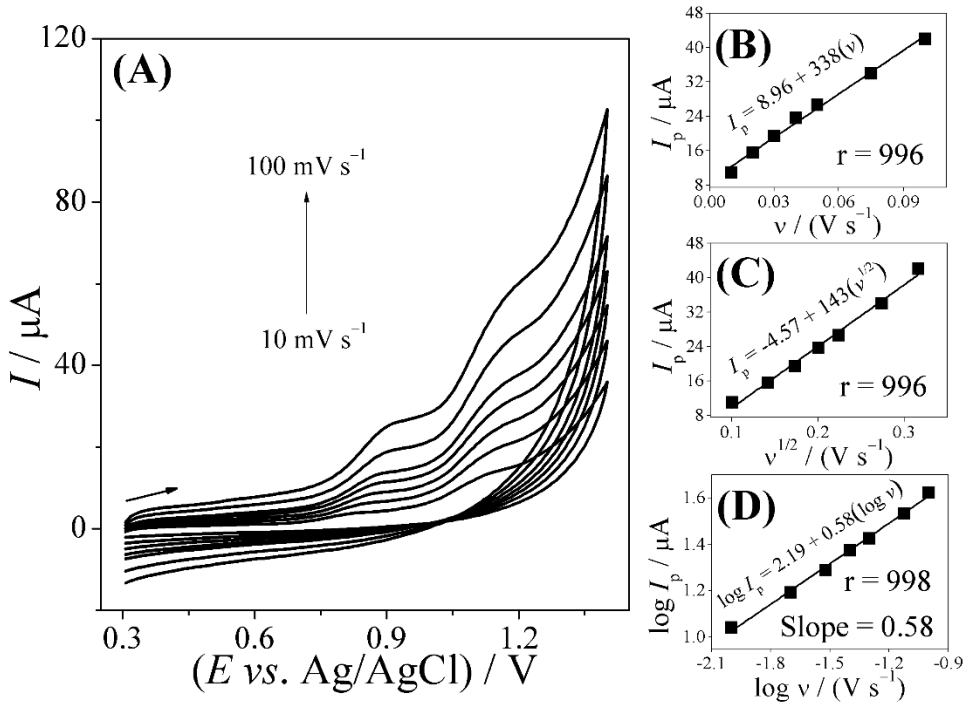

Fig. 5. (A) Cyclic voltammograms for different scan rates (10 - 100 mV s^{-1}) using the Pt NPs-MWCNTs/CPE sensor for 0.10 mmol L^{-1} HCQ in 0.10 mol L^{-1} PBS (pH 6.0), **(B)** ΔI_p *vs.* v, **(C)** ΔI_p *vs.* $v^{1/2}$ and **(D)** log ΔI_p *vs.* log v.

3.7. HCQ determination

After optimizing the detection parameters, the HCQ molecule was quantified by SWV using the Pt NPs-MWCNTs/CPE sensor in a 0.10 mol L^{-1} PBS, at pH 6.0, after successive injections of a standard solution of the analyte. As shown in Fig. 6, a variation in the concentration of HCQ led to a linear increase in the peak current magnitude (n = 3), evidencing the robustness of the proposed methodology.

The calibration curve profile (inset Fig. 6) showed a highly linear analytical response (r = 0.996) within the range of 0.099 to 7.1 µmol L^{-1}, with limit of detection (LOD) and limit of quantification (LOQ) of 28 nmol L^{-1} and 93 nmol L^{-1}, respectively. The LOD and LOQ values were calculated based on the following established statistical criteria: LOD = "3σ" / "S" and LOQ = "10σ" / "S", where σ represents the standard deviation of ten measurements of the blank signal (supporting electrolyte, n = 10), and S

corresponds to the slope of the calibration curve [48-50]. The analytical equation (Eq. 4) derived from linear regression demonstrated excellent fit, reaffirming the ability of the sensor to provide reproducible and highly sensitive results when applied for the detection of HCQ at low concentrations.

$$I_p(\mu A) = 0.075 + 0.20[HCQ]\ (\mu mol\ L^{-1}) / r = 0.996 \qquad \text{(Eq. 4)}$$

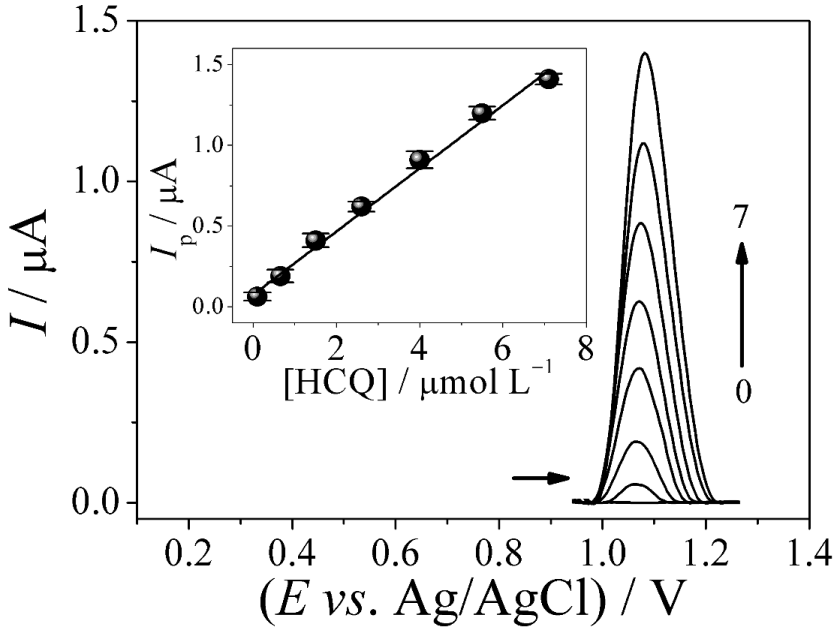

Fig. 6. SW voltammograms obtained using the Pt NPs-MWCNTs/CPE sensor in 0.10 mol L^{-1} PBS at pH 6.0 containing different concentrations for HCQ: (0 - 7) 0, 0.099, 0.65, 1.5, 2.6, 4.0, 5.5 and 7.1 μmol L^{-1}. Inset: analytical curve (n = 3). SWV parameters: a = 50 mV, f = 15 Hz, ΔE_s = 5 mV, and t_{acc} = 30 s.

Table 1 presents the data related to the analytical performance of the proposed Pt NPs-MWCNTs/CPE-based voltammetric method in comparison with other methods reported in the literature for HCQ detection [51,23,52,53,44,54,55]. As demonstrated, the Pt NPs-MWCNTs/CPE sensor exhibited comparable results in terms of sensitivity or

linear concentration range. Among the main advantages of the Pt NPs-MWCNTs/CPE sensor include its high selectivity, ease of preparation, and excellent repeatability and reproducibility, as proven in further analyses reported in this work.

These results help consolidate the proposed method as a suitable alternative for use in the electrochemical detection of HCQ; the method is particularly relevant in analytical environments where accuracy and robustness are crucial. The modification of the CPE with Pt NPs and MWCNTs not only enhances the sensor capacity and efficiency when applied for the detection of analytes at ultratrace levels but also offers significant gains in terms of stability and reliability of the results, thus positioning this sensor to be promising sensing devices for analytical applications.

Table 1 – Comparison between electroanalytical methods for HCQ detection.

Electrode	Method	Linear range (μmol L^{-1})	LOD (nmol L^{-1})	Sample	Ref.
3D-CB/PLA	SWV	0.4 – 7.5	40	Pharmaceutical, and tap water	[23]
SPCB/GCE	LSV	0.10 – 10.0	9.3	Pharmaceutical	[44]
BDD	SWV	0.1 – 1.9	60	Pharmaceutical, and urine	[51]
rGO-TiO_2/GCE	SWV	0.25 – 500	12.5	Pharmaceutical, and urine	[52]
MWCNTs/CPE	AdSDPV	0.057 – 100	6.0	Pharmaceutical, and Serum	[53]
GC-PMPDA SAM	DPV	0.09–10.21	4.65	Serum	[54]
ZnSNPs/rGO/ GCE	DPV	0.005–0.07	0.456	Plasma and urine	[55]
Pt NPs-MWCNTs/CPE	SWV	0.099 – 7.1	28	River water, synthetic urine, and bovine serum	This work

DPV: Differential Pulse Voltammetry; GCE: Glassy Carbon Electrode; rGO: Reduced Graphene Oxide; BDD: Boron Doped Diamond; AdSDPV: Adsorptive Stripping Differential Pulse Voltammetry; LSV: Linear Sweep Voltammetric; PMPDA: N,N′-bis[(E)-(1-pyridyl) methylidene]-1,3-propanediamine; SAM: self-assembled monolayer; ZnSNPs: Zinc sulfide nanoparticles; CB: Carbon black.

447 *3.8. Repeatability, reproducibility and selectivity studies*

448 The performance of the Pt NPs-MWCNTs/CPE sensor in terms of repeatability,
449 reproducibility, and selectivity was evaluated by the SWV technique using 0.10 mol L^{-1}
450 PBS, at pH 6.0, as supporting electrolyte, in the presence of 6.0 μmol L^{-1} HCQ. In the
451 repeatability tests, a single electrode was used for the conduct of ten consecutive
452 electrochemical measurements (*n = 10*), which yielded a relative standard deviation
453 (RSD) of 2.1% (Fig. S3A). This low RSD value points to the high degree of accuracy of
454 the proposed method for HCQ quantification. Subsequently, the reproducibility of the
455 sensor was analyzed after the renewal and polishing of each electrode surface (*n = 5*),
456 where an RSD of 2.0 % was obtained (Fig. S3B). The results obtained point to the
457 excellent stability and robustness of the sensor, even after the surface renewal procedures;
458 this is clearly essential when it comes to the use of the sensor for repetitive analyses.

459 The selectivity of the sensor was analyzed through the application of potential
460 interferents such as uric acid, glucose, urea, ascorbic acid, albumin, metals (Cd^{2+}, Pb^{2+}
461 and Zn^{2+}), and humic acid, using analyte to interferent concentration ratio of 1:10 (Fig.
462 S4). The error values obtained ranged between −3.7 and +1.7% in all tests (Table S2).
463 These findings suggest that the proposed Pt NPs-MWCNTs/CPE–based method is highly
464 selective for HCQ detection even in the presence of interferents at significantly higher
465 concentrations.

466

467 *3.9. HCQ detection in environmental and biological samples*

468 To evaluate the effectiveness of the proposed method, the Pt NPs-MWCNTs/CPE
469 sensor was used to quantify HCQ in environmental and biological samples. The tested
470 samples included river water, serum and synthetic urine, which were spiked with two
471 known concentrations of HCQ (0.60 and 4.0 μmol L^{-1}) for analysis (Fig. S5). The

recovery rates obtained from this analysis ranged from 92 to 105% (n = 3) (Table 2); these results show that the proposed method is capable of accurately quantifying HCQ in different sample types without significant matrix interference.

Table 2 – Results obtained using Pt NPs-MWCNTs/CPE sensor in the HCQ detection in different samples.

Samples	Added	Proposed method*	Comparative method*	Recovery** (%)	Error*** (%)
River water	6.0×10^{-7}	$(5.8 \pm 0.2) \times 10^{-7}$	$(6.1 \pm 0.3) \times 10^{-7}$	97	−4.9
	4.0×10^{-6}	$(4.1 \pm 0.1) \times 10^{-6}$	$(3.9 \pm 0.2) \times 10^{-6}$	102	5.1
Synthetic urine	6.0×10^{-7}	$(6.1 \pm 0.2) \times 10^{-7}$	$(6.3 \pm 0.1) \times 10^{-7}$	100	−3.2
	4.0×10^{-6}	$(4.2 \pm 0.1) \times 10^{-6}$	$(4.1 \pm 0.1) \times 10^{-6}$	105	2.4
Bovine serum	6.0×10^{-7}	$(5.5 \pm 0.3) \times 10^{-7}$	$(6.0 \pm 0.2) \times 10^{-7}$	92	−8.3
	4.0×10^{-6}	$(3.8 \pm 0.2) \times 10^{-6}$	$(4.1 \pm 0.3) \times 10^{-6}$	95	−7.3

*Average of 3 measured concentrations;
**Recovery percentage (proposed method) = [Found] / [Added] × 100;
***Error = [(Proposed method − Comparative method) / (Comparative method)] × 100.

Finally, as shown in Table 2, the samples were also analyzed using spectrophotometry - a standard reference method, the results of which were compared with those of the proposed method. This comparative analysis showed that the error between the two techniques ranged from –8.3% to 5.1%. In addition, the results obtained under both methods were statistically analyzed using the paired Student's *t*-test with a 95% confidence level. The calculated experimental value was 0.24, which is below the critical limit of 2.6; this shows that there is no statistically significant difference between the results obtained from the two analytical methods. Thus, these findings clearly point to the effectiveness of the Pt NPs-MWCNTs/CPE sensor when applied for HCQ detection in river water, synthetic urine and serum samples.

4. Conclusion

The data obtained from this study show that the application of the Pt NPs-MWCNTs/CPE sensor resulted in a significant increase in electrochemical signal for HCQ detection in low concentration. The modification of the CPE with Pt NPs-MWCNTs provided the electrode with high sensitivity, selectivity, and accuracy over a range of concentration from 0.099 to 7.1 μmol L^{-1}. The proposed sensor was found to be reliable and highly efficient when applied for HCQ quantification in environmental and biological samples, where it recorded recovery rates close to 100%. Thus, the methodology proposed in this study is a highly promising, robust alternative tool for HCQ monitoring, with great potential for use in a wide range of analytical applications in matrices of interest.

Acknowledgements The authors gratefully acknowledge the financial support granted by the São Paulo Research Foundation – FAPESP (grants #2019/06650-3, #2022/12895-1, #2022/05454-9 and #2023/14335-6) and CNPq (grants #303943/2021-1 and #102213/2024-0).

Conflicts of Interest: The authors have no conflict of interest to declare.

References

1. Kaur H., Siwal S. S., Chauhan G., Saini A. K., Kumari A., Thakur V. K. (2022). Recent advances in electrochemical-based sensors amplified with carbon-based nanomaterials (CNMs) for sensing pharmaceutical and food pollutants. *Chemosphere, 304*, 135182, doi:https://doi.org/10.1016/j.chemosphere.2022.135182.
2. Baranwal J., Barse B., Gatto G., Broncova G., Kumar A. (2022). Electrochemical Sensors and Their Applications: A Review. *Chemosensors, 10*(9), 363.
3. Singh R., Gupta R., Bansal D., Bhateria R., Sharma M. (2024). A Review on Recent Trends and Future Developments in Electrochemical Sensing. *ACS Omega, 9*(7), 7336-7356, doi:10.1021/acsomega.3c08060.
4. Ramya M., Senthil Kumar P., Rangasamy G., Uma shankar V., Rajesh, G., Nirmala K., et al. (2022). A recent advancement on the applications of nanomaterials in electrochemical

sensors and biosensors. *Chemosphere, 308*, 136416, doi:https://doi.org/10.1016/j.chemosphere.2022.136416.

5. Ibrahim M., Ibrahim H., Almandil N., Kawde, A.-N. (2018). Gold nanoparticles/f-MWCNT nanocomposites modified glassy carbon paste electrode as a novel voltammetric sensor for the determination of cyproterone acetate in pharmaceutical and human body fluids. *Sensors and Actuators B: Chemical, 274*, 123-132, doi:https://doi.org/10.1016/j.snb.2018.07.105.
6. Santos A. M., Wong A., Feitosa M. H. A., Cardenas-Riojas A. A., Calderon-Zavalet S. L., Baena-Moncada, A. M., et al. (2023). Voltammetric Sensing of Nifedipine Using a Glassy Carbon Electrode Modified with Carbon Nanofibers and Gold Nanoparticles. *Biosensors, 13*(8), 829.
7. Wong A., Santos A. M., Proença C. A., Baldo T. A., Feitosa M. H. A., Moraes F. C., et al. (2022). Voltammetric Determination of 3-Methylmorphine Using Glassy Carbon Electrode Modified with rGO and Bismuth Film. *Biosensors, 12*(10), 860.
8. Santos A. M., Feitosa M. H. A., Wong A., Fatibello-Filho O., Sotomayor M. D. P. T., Moraes F. C. (2024). Functionalized graphene, quantum dots, and PEDOT:PSS based screen-printed electrode for the endocrine disruptor bisphenol A determination. *Sensors and Actuators B: Chemical, 399*, 134745, doi:https://doi.org/10.1016/j.snb.2023.134745.
9. Sukanya, Kumara Swamy B. E., Shashikumara J. K., Sharma S. C. (2022). Poly (yellow PX4R) carbon paste electrode sensor for paracetamol: A voltammetric study. *Inorganic Chemistry Communications, 140*, 109394, doi:https://doi.org/10.1016/j.inoche.2022.109394.
10. Harsini M., Widyaningrum B. A., Fitriany E., Paramita D. R. A., Farida A. N., Baktir A., et al. (2022). Electrochemical synthesis of polymelamine/gold nanoparticle modified carbon paste electrode as voltammetric sensor of dopamine. *Chinese Journal of Analytical Chemistry, 50*(4), 100052, doi:https://doi.org/10.1016/j.cjac.2022.100052.
11. Madhuchandra H. D., Swamy B. E. K. (2020). Electrochemical determination of Adrenaline and Uric acid at 2-Hydroxybenzimidazole modified carbon paste electrode Sensor: A voltammetric study. *Materials Science for Energy Technologies, 3*, 464-471, doi:https://doi.org/10.1016/j.mset.2020.02.006.
12. Haghighi M., Rezaei M., Sariaslani P., Moradi S., Shahlaei, M. (2021). Sensitive electrochemical sensor for lamotrigine based on modified carbon paste electrode. *Monatshefte für Chemie - Chemical Monthly, 152*(8), 903-914, doi:10.1007/s00706-021-02811-w.
13. Hareesha N., Manjunatha J. G. (2020). Fast and enhanced electrochemical sensing of dopamine at cost-effective poly(DL-phenylalanine) based graphite electrode. *Journal of Electroanalytical Chemistry, 878*, 114533, doi:https://doi.org/10.1016/j.jelechem.2020.114533.
14. Gooding J. J. (2005). Nanostructuring electrodes with carbon nanotubes: A review on electrochemistry and applications for sensing. *Electrochimica Acta, 50*(15), 3049-3060, doi:https://doi.org/10.1016/j.electacta.2004.08.052.
15. Trojanowicz M. (2006). Analytical applications of carbon nanotubes: a review. *TrAC Trends in Analytical Chemistry, 25*(5), 480-489, doi:https://doi.org/10.1016/j.trac.2005.11.008.
16. Wang J. (2005). Carbon-Nanotube Based Electrochemical Biosensors: A Review. *Electroanalysis, 17*(1), 7-14, doi:https://doi.org/10.1002/elan.200403113.
17. Mazzotta E., Di Giulio T., Mastronardi V., Pompa P. P., Moglianetti M., Malitesta C. (2021). Bare Platinum Nanoparticles Deposited on Glassy Carbon Electrodes for Electrocatalytic Detection of Hydrogen Peroxide. *ACS Applied Nano Materials, 4*(8), 7650-7662, doi:10.1021/acsanm.1c00754.
18. Yang Y., Zeng Y., Tang C., Zhu X., Lu X., Liu L., et al. (2018). Voltammetric determination of 5-hydroxytryptamine based on the use of platinum nanoparticles coated with

molecularly imprinted silica. *Microchimica Acta, 185*(4), 219, doi:10.1007/s00604-018-2755-0.

19. Paczosa-Bator B., Piech R., Wardak C., Cabaj L. (2018). Application of graphene supporting platinum nanoparticles layer in electrochemical sensors with potentiometric and voltammetric detection. *Ionics, 24*(8), 2455-2464, doi:10.1007/s11581-017-2356-7.
20. Kalambate P. K., Srivastava A. K. (2016). Simultaneous voltammetric determination of paracetamol, cetirizine and phenylephrine using a multiwalled carbon nanotube-platinum nanoparticles nanocomposite modified carbon paste electrode. *Sensors and Actuators B: Chemical, 233*, 237-248, doi:https://doi.org/10.1016/j.snb.2016.04.063.
21. Jain U., Gupta S., Chauhan N. (2017). Detection of glycated hemoglobin with voltammetric sensing amplified by 3D-structured nanocomposites. *International Journal of Biological Macromolecules, 101*, 896-903, doi:https://doi.org/10.1016/j.ijbiomac.2017.03.127.
22. Monsef R., Salavati-Niasari M. (2022). Electrochemical sensor based on a chitosan-molybdenum vanadate nanocomposite for detection of hydroxychloroquine in biological samples. *Journal of Colloid and Interface Science, 613*, 1-14, doi:https://doi.org/10.1016/j.jcis.2022.01.039.
23. Carvalho M. S., Rocha R. G., de Faria L. V., Richter E. M., Dantas L. M. F., da Silva I. S., et al. (2022). Additively manufactured electrodes for the electrochemical detection of hydroxychloroquine. *Talanta, 250*, 123727, doi:https://doi.org/10.1016/j.talanta.2022.123727.
24. Oliveira-Ferreira J., Lacerda M. V. G., Brasil P., Ladislau J. L. B., Tauil P. L., Daniel-Ribeiro C. T. (2010). Malaria in Brazil: an overview. *Malaria Journal, 9*(1), 115, doi:10.1186/1475-2875-9-115.
25. Ferreira M. U., Castro M. C. (2016). Challenges for malaria elimination in Brazil. *Malaria Journal, 15*(1), 284, doi:10.1186/s12936-016-1335-1.
26. Carlos B. C., Rona L. D. P., Christophides G. K., Souza-Neto J. A. (2019). A comprehensive analysis of malaria transmission in Brazil. *Pathogens and Global Health, 113*(1), 1-13, doi:10.1080/20477724.2019.1581463.
27. Bajpai J., Pradhan A., Verma A. K., Kant, S. (2022). Use of hydroxychloroquine and azithromycin combination to treat the COVID-19 infection. *World J Exp Med, 12*(3), 44-52, doi:10.5493/wjem.v12.i3.44.
28. Beltran Gonzalez J. L., González Gámez M., Mendoza Enciso E. A., Esparza Maldonado R. J., Hernández Palacios D., Dueñas Campos S., et al. (2022). Efficacy and Safety of Ivermectin and Hydroxychloroquine in Patients with Severe COVID-19: A Randomized Controlled Trial. *Infectious Disease Reports, 14*(2), 160-168. doi:10.3390/idr14020020
29. Ben-Zvi I., Kivity S., Langevitz P., Shoenfeld Y. (2012). Hydroxychloroquine: from malaria to autoimmunity. *Clin Rev Allergy Immunol, 42*(2), 145-153, doi:10.1007/s12016-010-8243-x.
30. Sotgia S., Zinellu A., Mundula N., Mangoni A. A., Carru C., Erre G. L. (2022). A Capillary Electrophoresis-Based Method for the Measurement of Hydroxychloroquine and Its Active Metabolite Desethyl Hydroxychloroquine in Whole Blood in Patients with Rheumatoid Arthritis. *Molecules, 27*(12), 3901.
31. Shrivastava A. (2020). Analytical methods for the determination of hydroxychloroquine in various matrices. *Int. J. Appl. Pharm, 4*, 55-61.
32. Ramzy S., Abdelazim A. H., Osman A. O. E., Hasan M. A. (2022). Spectrofluorimetric quantitative analysis of favipiravir, remdesivir and hydroxychloroquine in spiked human plasma. *Spectrochimica Acta Part A: Molecular and Biomolecular Spectroscopy, 281*, 121625, doi:https://doi.org/10.1016/j.saa.2022.121625.
33. Xiong X., Wang K., Tang T., Fang J., Chen Y. (2021). Development of a chiral HPLC method for the separation and quantification of hydroxychloroquine enantiomers. *Sci Rep, 11*(1), 8017, doi:10.1038/s41598-021-87511-5.

34. Qu Y., Noe G., Breaud A. R., Vidal M., Clarke W. A., Zahr N., et al. (2015). Development and validation of a clinical HPLC method for the quantification of hydroxychloroquine and its metabolites in whole blood. *Future Science OA, 1*(3), FSO26, doi:10.4155/fso.15.24.
35. Mohammadzadeh Jahani P., Tajik S., Beitollahi H., Garkani Nejad F., Dourandish, Z. (2024). Determination of Methotrexate Using an Electrochemical Sensor Based on Carbon Paste Electrode Modified with NiO Nanosheets and Ionic Liquid. *Chemosensors, 12*(12), 266.
36. Ganjali M. R., Nejad F. G., Beitollahi H., Jahani S., Rezapour M., Larijani B. (2017). Highly Sensitive Voltammetric Sensor for Determination of Ascorbic Acid Using Graphite Screen Printed Electrode Modified with ZnO/Al2O3 Nanocomposite. *International Journal of Electrochemical Science, 12*(4), 3231-3240, doi:https://doi.org/10.20964/2017.04.07.
37. Singh K., Maurya K. K., Malviya M. (2024). Review of Electrochemical Sensors and Biosensors Based on First-Row Transition Metals, Their Oxides, and Noble Metals Nanoparticles. *Journal of Analysis and Testing, 8*(2), 143-159, doi:10.1007/s41664-023-00292-w.
38. Deng H.-H., Lin X.-L., Liu Y.-H., Li K.-L., Zhuang Q.-Q., Peng H.-P., et al. (2017). Chitosan-stabilized platinum nanoparticles as effective oxidase mimics for colorimetric detection of acid phosphatase. [10.1039/C7NR03399K]. *Nanoscale, 9*(29), 10292-10300, doi:10.1039/C7NR03399K.
39. Wong A., Sotomayor, M. D. P. T. (2013). Biomimetic sensor based on 5,10,15,20-tetrakis(pentafluorophenyl)-21H,23H-porphyrin iron (III) chloride and MWCNT for selective detection of 2,4-D. *Sensors and Actuators B: Chemical, 181*, 332-339, doi:https://doi.org/10.1016/j.snb.2012.12.095.
40. Laube N., Mohr B., Hesse A. (2001). Laser-probe-based investigation of the evolution of particle size distributions of calcium oxalate particles formed in artificial urines. *Journal of Crystal Growth, 233*(1), 367-374, doi:https://doi.org/10.1016/S0022-0248(01)01547-0.
41. Bard A. J., Faulkner L. R. (2001). *Electrochemical Methods: Fundamentals and Applications* (Vol. 2). New York: John Wiley & Sons Inc.
42. Trachioti M. G., Lazanas A. C., Prodromidis M. I. (2023). Shedding light on the calculation of electrode electroactive area and heterogeneous electron transfer rate constants at graphite screen-printed electrodes. *Microchimica Acta, 190*(7), 251, doi:10.1007/s00604-023-05832-w.
43. Randviir E. P. (2018). A cross examination of electron transfer rate constants for carbon screen-printed electrodes using Electrochemical Impedance Spectroscopy and cyclic voltammetry. *Electrochimica Acta, 286*, 179-186, doi:https://doi.org/10.1016/j.electacta.2018.08.021.
44. Silva J. P. C., Santos-Neto D. R., Lopes C. E. C., Silva L. R. G., Dantas L. M. F., da Silva I. S. (2024). A high sensitivity adsorptive-electrochemical method for rapid and portable determination of hydroxychloroquine. *Journal of Solid State Electrochemistry*, doi:10.1007/s10008-024-06032-z.
46. Mater Mahnashi H., Mahmoud A. M., Saad Alkahtani A., El-Wekil M. M. (2021). Simultaneous electrochemical detection of azithromycin and hydroxychloroquine based on VS2 QDs embedded N, S @graphene aerogel/cCNTs 3D nanostructure. *Microchemical Journal, 163*, 105925, doi:https://doi.org/10.1016/j.microc.2021.105925.
47. Wong A., Santos A. M., Fatibello-Filho O. (2018). Simultaneous determination of paracetamol and levofloxacin using a glassy carbon electrode modified with carbon black, silver nanoparticles and PEDOT:PSS film. *Sensors and Actuators B: Chemical, 255*, 2264-2273, doi:https://doi.org/10.1016/j.snb.2017.09.020.

48. Nic M., Hovorka L., Jirat J., Kosata B., Znamenacek J. (2005). *IUPAC compendium of chemical terminology-the gold book*: International Union of Pure and Applied Chemistry.
49. Skoog D. A., Holler F. J., Crouch S. R. (2019). Textbook" principles of instrumental analysis.". *Cengage learning. core. ac. uk. https://core. ac. uk/download/pdf/232277508. pdf*.
50. Food F. (2001). Guidance for industry: bioanalytical method validation. *http://www. fda. gov/cder/Guidance/4252fnl. pdf*.
51. Deroco P. B., Vicentini F. C., Oliveira G. G., Rocha-Filho R. C., Fatibello-Filho O. (2014). Square-wave voltammetric determination of hydroxychloroquine in pharmaceutical and synthetic urine samples using a cathodically pretreated boron-doped diamond electrode. *Journal of Electroanalytical Chemistry, 719*, 19-23, doi:https://doi.org/10.1016/j.jelechem.2014.01.037.
52. Huilan Z., Cheng L., Shang H., Zhang W., Zhang A. (2021). A Novel Electrochemical Sensor Based on Reduced Graphene Oxide–TiO2 Nanocomposites with High Selectivity for the Determination of Hydroxychloroquine. *Russian Journal of Electrochemistry, 57*(8), 872-884, doi:10.1134/S1023193521080152.
53. Ghoreishi S. M., Attaran A. M., Amin A. M., Khoobi A. (2015). Multiwall carbon nanotube-modified electrode as a nanosensor for electrochemical studies and stripping voltammetric determination of an antimalarial drug. [10.1039/C4RA16357E]. *RSC Advances, 5*(19), 14407-14415, doi:10.1039/C4RA16357E.
54. Khoobi A., Ghoreishi S. M., Behpour M., Shaterian M., Salavati-Niasari M. (2014). Design and evaluation of a highly sensitive nanostructure-based surface modification of glassy carbon electrode for electrochemical studies of hydroxychloroquine in the presence of acetaminophen. *Colloids and Surfaces B: Biointerfaces, 123*, 648-656, doi:https://doi.org/10.1016/j.colsurfb.2014.10.002.
55. Alkahtani S. A., Mahmoud A. M., Mahnashi M. H., AlQarni A. O., Alqahtani Y. S. A., El-Wekil M. M. (2021). Facile one pot sonochemical synthesis of layered nanostructure of ZnS NPs/rGO nanosheets for simultaneous analysis of daclatasvir and hydroxychloroquine. *Microchemical Journal, 164*, 105972, doi:https://doi.org/10.1016/j.microc.2021.105972.